CHEMIJA
2026. Vol. 37. No. 2. P. 90–107

ISSN 0235-7216 eISSN 2424-4538
DOI: https://doi.org/10.6001/chemija.2026.37.2.2

Comparative evaluation of phenolic composition, enzymes inhibition, antimicrobial virulence and chemical antioxidant activities of *Atriplex halimus* L. (Amaranthaceae) from mining and non-mining sites in Eastern Algeria

Khaled Rais[1],

Louiza Boudiba[1],

Sameh Boudiba[1],

Alfred Ngenge Tamfu[3, 5, 6*],

Baya Berka[2],

Selcuk Kucukaydin[3, 4],

Ozgur Ceylan[5],

Karima Hanini[1]

[1] *Laboratory of Applied Chemistry and Renewable Energies (LACRE), Echahid Cheikh Larbi Tebessi University, Tebessa, Algeria*

[2] *Animal Biology and Physiology Research Laboratory (LBPA), Higher Teacher Training School of Kouba, Vieux Kouba, BP 92, Algeria*

[3] *Department of Chemistry, Faculty of Science, Mugla Sitki Kocman University, 48000 Kotekli, Mugla, Turkey*

[4] *Department of Medical Services and Techniques, Koycegiz Vocational School of Health Services, Mugla Sitki Kocman University, P.O. Box 48800 Mugla, Turkey*

[5] *Food Quality Control and Analysis Program, Ula Ali Kocman Vocational School, Mugla Sitki Kocman University, Mugla 48147, Turkey*

[6] *Department of Chemical Engineering, School of Chemical Engineering and Mineral Industries, University of Ngaoundere, Ngaoundere 454, Cameroon*

Mining dust can enter plant tissues and impair phytosynthesis, nutrient uptake and production of secondary metabolites. This study investigates a comparative study of phenolic compounds and bioactivities of *Atriplex halimus* from mining (Ouenza) and non-mining (Tebessa City) sites. Chemical profiling and bioassays suggest that mining-associated environmental stress, including iron dust exposure, influences the plant's metabolism. HPLC-DAD phenolic profile revealed that amounts of p-hydroxybenzoic acid, *p*-coumaric acid, caffeic acid and taxifolin decreased with exposure to mining dust while syringic acid, vanillin, ferulic acid, quercetin, rutin, luteolin and catechin increased upon exposure to mining dust. The antimicrobial activity of the samples was low to moderate and varied from 0.3125 to 5 mg/mL. The plant fractions equally inhibited biofilm formation against *S. aureus*, *E. coli* and *C. albicans* with *S. aureus* being the most susceptible. All fractions inhibited violacein production in *C. violaceum* CV12472 at MIC, MIC/2 and MIC/4 and equally showed quorum-sensing inhibition zones against *C. violaceum* CV026, with the fractions from non-mining sites being more potent. The plant fractions exhibited inhibitory effects varying from 17.95 ± 0.20 to 52.70 ± 0.31% at 200 μg/mL on acetylcholinesterase (AChE) and butyrylcholinesterase (BChE), suggesting their potential in relieving symptoms of Alzheimer's disease. The fractions exhibited a low to moderate inhibition of α-glucosidase and α-amylase ranging from 13.44 ± 0.88 to 49.41 ± 0.65% at 200 μg/mL. Interestingly, the mining iron dust seems to have induced oxidative stress which triggered a compensatory increase in phenolic antioxidants, as confirmed by cyclic voltammetry. This research gives insights into the understanding of plant resilience in polluted environments, and effects on plant metabolism.

Keywords: *Atriplex halimus* L., phenolic profile, quorum-sensing inhibition, antibiofilm activity, enzyme inhibition, cyclic voltammetry

* Corresponding author. Email: macntamfu@yahoo.co.uk

INTRODUCTION

The negative impacts of mining on plants and animals as well as the environmental air, land and water resources are undeniable though mining itself is necessary for economic growth and development [1]. Mining dust can have a detrimental effect on plants, through disrupting vital functions including transpiration, photosynthesis and nutrient uptake, resulting in stunted growth, decreased production, and even plant death [2]. Besides containing elements that can be toxic to plants, mining dust also creates changes in the soil chemistry and making some relevant nutrients less available to plants [3]. Mining dust deposits on leaves block stomata and transpiration, resulting in reduced sunlight and photosynthesis as well as increased overheating, dehydration of leaves and stress of the plant. Mining-related dust can modify plant physiological function and communities, decrease plant cover, and increase metal concentrations in vegetation, thereby impacting the quantity, kind, quality and survivorship of forage [4, 5]. Mining activities, particularly in regions rich in iron deposits such as Eastern Algeria's Ouenza area, contribute to the release of dust particles that significantly affect the surrounding ecosystem, including plant life. This environmental challenge is particularly pertinent for plants, like *Atriplex halimus* L., a shrub native to arid and semi-arid regions known for its resilience to stressors such as a high salinity and drought [6]. Despite its robustness, the specific response of *A. halimus* to pollutants, especially those associated with mining dust, remains understudied. This highlights the need for further research into how this species adapts to such conditions, which could provide valuable insights into its potential role in mitigating the environmental impacts of mining activities. The Ouenza region is characterised by its iron mining activities [7], which presents a unique opportunity to study how this environmental stress influences plant chemistry and biological functions. The plant's ability to tolerate such pollutants may provide valuable insights into natural defence mechanisms [8], such as the production of secondary metabolites, including phenolic compounds, which are known for their antioxidant [9], antibacterial properties [10], and modulating renal function damage [11, 12]. These compounds play a critical role in mitigating oxidative stress [13], a common consequence of exposure to heavy metals and other pollutants [14–16].

This study aims to investigate the effects of mining iron dust on *Atriplex halimus* L. by comparing samples collected from Ouenza (W) with mining activities and those collected from Tebessa City (T), a nearby location without mining activities. The research focuses on understanding changes in the plant's chemical composition and biological activities and correlating these findings with iron dust. The ultimate goal is to enhance our understanding of plant responses to environmental pollutants and inform strategies for ecological management, especially in mining-impacted areas. Additionally, the findings may contribute to broader efforts to preserve plant biodiversity, protect agricultural productivity, and promote human health by mitigating the harmful effects of mining pollution.

MATERIALS AND METHODS

Study area and plant material

The Ouenza iron mine in Northeastern Algeria is a significant source of airborne particulate matter, adversely impacting air quality and environmental health [17, 18]. Mining activities such as drilling, blasting, excavation, loading, crushing and transportation contribute significantly to dust emissions. These emissions are exacerbated by the region's arid climatic conditions, low humidity and prevailing winds, particularly in the southern sector of the mine [19]. The mine comprises seven opencast sites with varied altitudinal ranges, influencing particulate dispersal due to meteorological variations at different elevations [20]. Unpaved haul roads and conveyor belts used for ore transport further amplify dust pollution [21]. Crushing operations at two primary stations release fine particulates, affecting workers and nearby populations if effective mitigation measures are not implemented [22]. Ouenza's geographical setting, exceeding 1200 m in altitude, alongside dry weather, intensifies particulate dispersal, creating significant environmental and health challenges. Dust control strategies are essential to address the adverse effects on ecosystems, vegetation, and public health [23]. *Atriplex halimus* L. plant material was properly identified and authenticated by Hioun Soraya, under the voucher specimen (AMA/5.2.3/HS) deposited at the Faculty of Exact Sciences, Natural Sciences,

and Life Sciences Laboratory or Echahid Cheikh Larbi Tebessi University. Aerial parts of the plant were harvested from two regions of Eastern Algeria: Ouenza (W) and Tébessa (T) (Fig. 1), during their flowering period in October 2023.

To minimise seasonal and phenological variability, all plant samples were collected during the same flowering stage and within the same harvesting period (October 2023). Although the investigated regions belong to the same broad semi-arid zone of Eastern Algeria, they differ in local climatic characteristics, particularly rainfall intensity, aridity level, and environmental exposure. Tebessa City presents intermediate semi-arid conditions, whereas Ouenza is relatively drier and additionally subjected to chronic mining-derived particulate emissions generated by extraction, crushing, drilling, and ore transportation activities. Previous studies on Atriplex halimus collected from the Saharan region of Negrine [86], characterised by stronger desert aridity, demonstrated that climatic drought alone can substantially influence phenolic metabolism. Therefore, the phytochemical and biological differences observed in the present work should be interpreted as adaptive responses to combined environmental pressures, including climatic stress and mining-associated oxidative stress.

Extraction

The plant material was initially shaded, dried, and then ground into a fine powder. A total of 700 g of the obtained material was extracted at room temperature using a methyl alcohol/water mixture (1:1), identified as the most effective solvent for extraction. After 24 h, the filtered extract was evaporated to yield a crude solid paste. Hot water was added to the paste, and the mixture was left to stand for 24 h before being filtered. The resulting aqueous extract was partitioned through liquid-liquid extraction using organic solvents, including dichloromethane (DCM), ethyl acetate (AcOEt) and n-butanol (BuOH). Each separated fraction was subsequently evaporated to dryness for further analysis. The percentage yield of each fraction was determined.

Determination of phenolic compounds

The phenolic compounds were identified using the HPLC-DAD method. For this analysis, the plant extracts were dissolved in a water-methanol (80:20) mixture, and the solution was filtered through a 0.20 µm disposable LC filter disk. Separation was accomplished on an Inertsil ODS-3 reverse phase C18 column [24, 25]. The flow rate was fixed at 1.0 mL/min with a 20-µL injection volume. Mobile phase A consisted of 0.5% acetic acid in water, and the mobile phase B contained 0.5% acetic acid in methanol. The gradient was as follows: 0–10% B (0–0.01 min); 10–20% B (0.01–5 min); 20–30% B (5–15 min); 30–50% B (15–25 min); 50–65% B (25–30 min); 65–75% B (30–40 min); 75–90% B (40–50 min); 90–10% B (50–55 min).

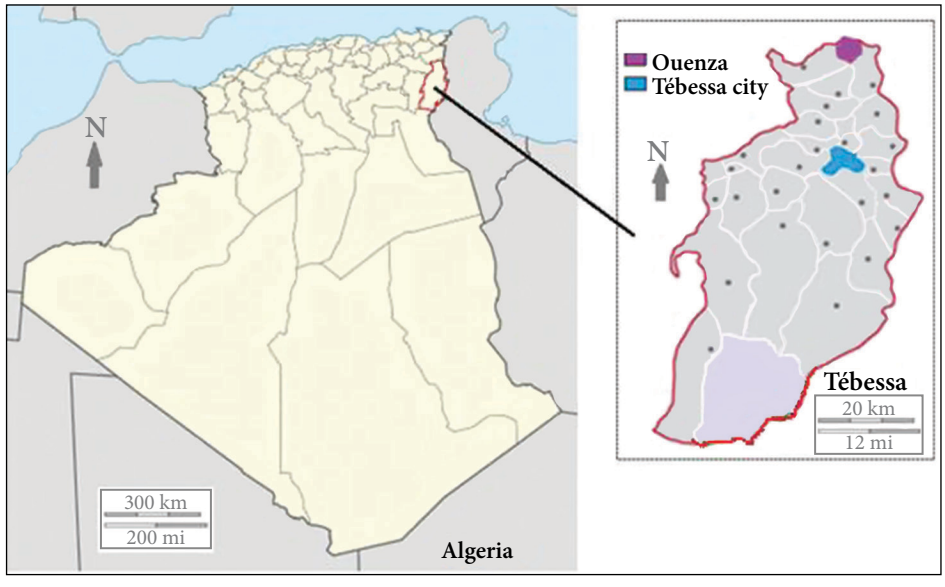

Fig. 1. Geographic situation of the site of plant collection

Detection was performed using a photodiode array detector (PDA) set to 280 nm. Polyphenols were identified by co-injection and comparison of retention times and UV data with known standards. The analysis was conducted in triplicate. To evaluate quantitatively the plant-contained compounds, a calibration curve was constructed using standard compound concentrations (0.0, 0.00782, 0.01563, 0.03125, 0.0625, 0.125, 0.25, 0.5 and 1.0 ppm). A total of 26 phenolic compounds were identified, including protocatechuic acid, gallic acid, chlorogenic acid, p-hydroxybenzoic acid, vanillic acid, 3-hydroxybenzoic acid, syringic acid, ferulic acid, p-coumaric acid, rosmarinic acid, ellagic acid, trans-cinnamic acid, pyrocatechol, vanillin, catechin, 6,7-dihydroxy-coumarin, coumarin, quercetin, rutin, luteolin, hesperetin, taxifolin, myricetin, apigenin, kaempferol and chrysin. The results are expressed in micrograms per gram of dry weight (μg/gDW).

Minimal inhibitory concentration (MIC) determination

The MIC was determined using the microliter broth dilution method, as described previously [26]. The MIC was defined as the lowest concentration of fraction that showed no visible bacterial growth. Mueller-Hinton Broth (MHB) was used as the test medium, and the bacterial density was set at 5×10^5 colony-forming units (CFU)/mL. 100 μL of bacterial suspensions were inoculated into the wells of a 96-well microliter plate, along with different final concentrations of the plant extract (5, 2.5, 1.25, 0.625, 0.3125… mg/mL) prepared in distilled water. The microplates were incubated at 37°C for 24 h before reading the results.

Violacein inhibition method using *C. violaceum* CV12472

Violacein production represents a quorum-sensing process and can be measured against *C. violaceum* CV12472 through qualitative analysis [27]. 10 μL of the overnight culture of *C. violaceum* was adjusted to 0.4 OD at 600 nm, added into sterile microplates containing 200 μL of LB broth, and then incubated in the absence and the presence of sub-MIC concentrations of the fractions prepared in distilled water. Broth with *C. violaceum* CV 12472 was used as a positive control. These plates were incubated for 24 h at 30°C when a diminution in the growth of violacein pigment was observed. The absorbance used for recording was 585 nm. Each experiment was realised in triplicate, and the violacein inhibition percent was calculated using the following formula:

$$\text{Violacein inhibition (\%)} = \frac{\text{OD 585 control-OD 585 sample}}{\text{OD 585 control}} \times 100.$$

Quorum-sensing inhibition (QSI) assay against *C. violaceum* CV026

The evaluation of quorum-sensing inhibition was done as described elsewhere [28]. Firstly, 5 mL of warm molten Soft Top Agar (2.0 g Tryptone, 1.3 g Agar agar, 1.0 g sodium chloride in 200 mL deionized water) was seeded with a 100 μL overnight culture of CV026. A 20 μL of C_6HSL was added as an exogenous AHL (Acyl Homoserine Lactone) source. This mixture was softly stirred and combined immediately over the surface of a solidified Luria Bertani Agar (LBA) plate as a film. A total of 5 mm in diameter of the wells was made after the solidification of the overlay on each plate. Each well was then filled with 50 μL of filter-sterilised extract solution in distilled water at a sub-MIC concentration. QSI is indicated as a cream or white-coloured halo around this well against a purple lawn of activated bacteria, CV026. The activity detection limit was made by employing serial dilutions of the extracts (from 1:1 to 1:8, using LB broth as diluent). The estimated endpoints were the lowest dilution of sample fractions, leading to the distinguishable inhibition of the synthesis of violacein pigment. Each experiment was realised in triplicate. The microplates were incubated for three days at 30°C, and then the quorum-sensing inhibition zone diameters were measured.

P. aeruginosa PA01 swarming motility inhibition assay

The swarming motility inhibition test was realised as previously described [29]. Shortly, *P. aeruginosa* PA01 strain overnight cultures were point inoculated at the centre of swarming plates containing 1% peptone, 0.5% agar, 0.5% NaCl and 0.5% filter-sterilised D-glucose with various sample extract concentrations (50, 75 and 100 μg/mL) in an aqueous solution. The plates were incubated in an upright position at an appropriate temperature for 18 h, and the control experiment was carried out

in the same way but without extracts. By following the bacterial cell swarm fronts, the swarming migration was recorded and used in calculating percentage inhibition with respect to the control.

Anticholinesterase activity

Spectrophotometry was used to measure the anticholinesterase activity by the enzymatic inhibition of the enzymes, acetylcholinesterase and butyrylcholinesterase, described elsewhere with slight modifications [30, 31]. Briefly, sodium phosphate buffer, 130 µL (100 mm, pH 8.0), 10 µL of sample extract solution, which was dissolved in ethanol in different concentrations, and buffer enzyme solution (AChE or BChE, 20 µL) were combined and incubated at 25°C for 15 min, and then 20 µL of 0.5 mM DTNB was added (5,5′-Dithiobis(2-nitrobenzoic) acid). The reaction was then initiated by the addition of acetylthiocholine iodide (20 µL, 0.71 mM) or butyrylthiocholine chloride (20 µL, 0.2 mM). The yellow 5-thio-2-nitrobenzoate anion formation in the reaction of DTNB with thiocholine, released by the enzymatic hydrolysis of butyrylthiocholine chloride or acetylthiocholine iodide, respectively, was monitored via spectrophotometry at a wavelength of 412 nm, using a 96-well microplate reader. The results were expressed as the enzyme inhibition percentage for 200 µg/mL extract concentration.

Bioassay of α-glucosidase and α-amylase inhibition

The antidiabetic potential of the extracts was measured through the inhibition of both α-glucosidase and α-amylase as described previously [31]. For the α-glucosidase assay, the extracts (1 mg/mL, 50 µL) were combined with 50 µL of glutathione (1 mg/mL, in phosphate buffer at pH 6.8) and 50 µL of substrate (PNPG, 10 mM). After a 15-minute incubation at 37°C, 50 µL of sodium carbonate was added to halt the reaction. The final absorbances were measured at 400 nm using a 96-well microplate reader, with acarbose serving as the positive standard. The data were expressed as the percentage of enzymatic inhibition at a concentration of 200 µg/mL.

To assess the α-amylase inhibition properties, the method described previously was employed [32]. 50 µL of the sample solution that had been dissolved in ethanol was mixed with 150 µL of a solution made by adding 1.5 mg of soluble starch to 150 µL of buffer solution (0.2 M, pH 6.8, 17 mM NaCl). Subsequently, 10 µL of α-amylase enzyme (25 units/mL) was incubated for 30 min at 37°C. After incubation, 20 µL of 2N NaOH and 20 µL of a colour reagent (comprising 3,5-dinitrosalicylic acid at 44 µM, potassium sodium tartrate tetrahydrate at 106 µM and NaOH at 40 µM) were introduced. A second incubation was carried out for 20 min at 100°C. The absorbance was measured at 540 nm, and the results were expressed as percentage inhibition at 200 µg/mL. Acarbose was used as the standard for comparison.

Chemical antioxidant assay

The measurements are carried out in a 25 mL electrochemical cell and a three-electrode system. The superoxide radical anion is generated by commercial molecular oxygen dissolved in DMF, which contains 0.1 M of NBu_4PF_6 at room temperature. The sweep rate is 100 mV/s. The applied potential range has been achieved from –1.6 to 0 V with respect to ECS. The electrochemical study of the behaviour of gallic acid and extracts of *Atriplex halimus* L. is carried out at a concentration of 0.1 mM, added in the electrochemical cell [33]. The ability of the tested product to scavenge superoxide radicals ($O_2^{\bullet -}$) is calculated using the equation

$$\text{Superoxide ion inhibiting capacity (\%)} = \frac{Ip_0 - Ip_s}{Ip_0} \times 100,$$

where Ip_0 is the current intensity of the anodic peak of oxygen alone, and Ip_s is the current intensity of the anodic peak of oxygen in the presence of plant fractions.

Statistical analysis

Each activity was performed in triplicate, and the results were recorded as the means ± standard error of the mean (SEM). Statistical analyses were conducted to identify significant differences between means, with a significance threshold set at $p < 0.05$.

RESULTS AND DISCUSSION

Extraction yield and HPLC-DAD phenolic composition of the *Atriplex halimus* L. fractions

Extraction is an important step for obtaining active compounds from plants and it depends on

the target compounds. The compounds of interest in this study are phenolic compounds. Using maceration with MeOH:H_2O (1:1) solvent mixture, and subsequent solvent:solvent partitioning, various fractions were obtained from *Atriplex halimus* L. aerial parts. The crude extract was re-extracted using liquid-liquid extraction in order of increasing polarity to afford dichloromethane (DCM), ethyl acetate (AcOEt), n-butanol (BuOH) and aqueous extract (Aq) of the plant material collected from Ouenza (W) and Tebessa (T). The percentage yield of each fraction is provided in Table 1. The best yield for all cases was for the aqueous fraction, followed by the butanol fraction, then dichloromethane, and the lowest yield was observed in the ethyl acetate fractions.

Table 1. **Extraction yield of the fractions of *A. halimus* L. plant material**

Solvent for crude extract	Extract fraction	Yield, %	
		W	T
MeOH/water (1:1)	DCM	0.24	0.22
	AcOEt	0.16	0.18
	BuOH	0.70	1.22
	H_2O (Aq)	20.06	19.38

Besides the extraction method, environmental conditions and other anthropogenic activities can affect the chemical content as well as the extraction yields of plants.

Phenolic compounds extracted from *Atriplex halimus* L. with various solvents were analysed using HPLC-DAD, and the results are summarised in Table 2. The structures of the major identified compounds detected are provided in Fig. 2. Chlorogenic acid, caffeic acid, ferulic acid, rutin and chrysin were found in all the fractions of the plant samples collected from both areas. Generally, the ethyl acetate and n-butanol fractions of plant samples from both areas had the highest amounts of phenolic compounds detected while the ethyl acetate fractions had the highest amounts of phenolic compounds quantified by HPLC-DAD. The AcOEt fraction of plant sample from the Ouenza area had significant amounts of caffeic acid (111.7 ± 0.30 μg/g), p-coumaric acid (57.30 ± 0.13 μg/g), ferulic acid (167.2 ± 0.40 μg/g) and rutin (76.27 ± 0.26 μg/g). The AcOEt fraction of plant sample from the Tebessa area had significant amounts of caffeic acid (122.5 ± 0.70 μg/g), p-coumaric acid (125.4 ± 0.35 μg/g), ferulic acid (79.84 ± 0.37 μg/g) and rutin (58.66 ± 0.45 μg/g).

Table 2. **Phenolic composition of *Atriplex halimus* L. extracts by HPLC-DAD (μg/g)[a]**

Phenolic compounds	RT, min	W-DCM	W-AcOEt	W-BuOH	W-Aq	T-DCM	T-AcOEt	T-BuOH	T-Aq
Catechin	10.68	–	14.64 ± 0.05	12.70 ± 0.15	08.18 ± 0.04	00.96 ± 0.07	17.260 ± 0.20	09.36 ± 0.14	–
Chlorogenic acid	12.35	02.20 ± 0.06	23.60 ± 0.32	06.54 ± 0.10	18.66 ± 0.11	01.40 ± 0.05	15.78 ± 0.16	04.16 ± 0.09	00.48 ± 0.05
p-Hydroxy benzoic acid	12.77	–	29.48 ± 0.21	03.95 ± 0.06	–	–	38.62 ± 0.33	08.08 ± 0.17	–
Caffeic acid	15.09	36.16 ± 0.18	111.7 ± 0.30	12.18 ± 0.14	04.82 ± 0.08	12.07 ± 0.16	122.5 ± 0.70	13.41 ± 0.21	02.61 ± 0.08
Syringic acid	16.56	38.63 ± 0.11	42.71 ± 0.29	11.84 ± 0.08	01.25 ± 0.05	29.25 ± 0.31	38.78 ± 0.17	06.67 ± 0.15	–
Vanillin	17.78	39.88 ± 0.27	24.70 ± 0.22	22.63 ± 0.13	01.86 ± 0.03	11.81 ± 0.25	14.63 ± 0.12	03.77 ± 0.08	–
p-Coumaric acid	20.56	–	57.30 ± 0.13	07.00 ± 0.17	–	–	125.4 ± 0.35	03.98 ± 0.06	–
Taxifolin	21.26	–	21.25 ± 0.17	07.32 ± 0.24	02.63 ± 0.07	–	25.40 ± 0.22	17.48 ± 0.35	03.95 ± 0.10
Ferulic acid	22.14	17.43 ± 0.15	167.2 ± 0.40	67.85 ± 0.38	44.50 ± 0.29	09.25 ± 0.17	79.84 ± 0.37	55.79 ± 0.42	16.41 ± 0.30
Rutin	25.30	81.35 ± 0.24	76.27 ± 0.26	33.31 ± 0.40	02.62 ± 0.03	18.58 ± 0.21	58.66 ± 0.45	23.90 ± 0.36	01.45 ± 0.06
Quercetin	30.83	03.38 ± 0.04	42.54 ± 0.15	59.78 ± 0.20	–	–	26.63 ± 0.31	01.45 ± 0.04	–
Luteolin	31.70	02.63 ± 0.05	26.68 ± 0.10	02.73 ± 0.05	–	01.48 ± 0.04	19.81 ± 0.20	01.38 ± 0.08	–
Chrysin	38.40	29.51 ± 0.12	38.54 ± 0.10	42.65 ± 0.15	32.12 ± 0.11	41.31 ± 0.27	52.20 ± 0.15	38.25 ± 0.15	28.08 ± 0.37

– : not detected. [a] Values expressed are means ± S.E.M. of three parallel measurements ($p < 0.05$).

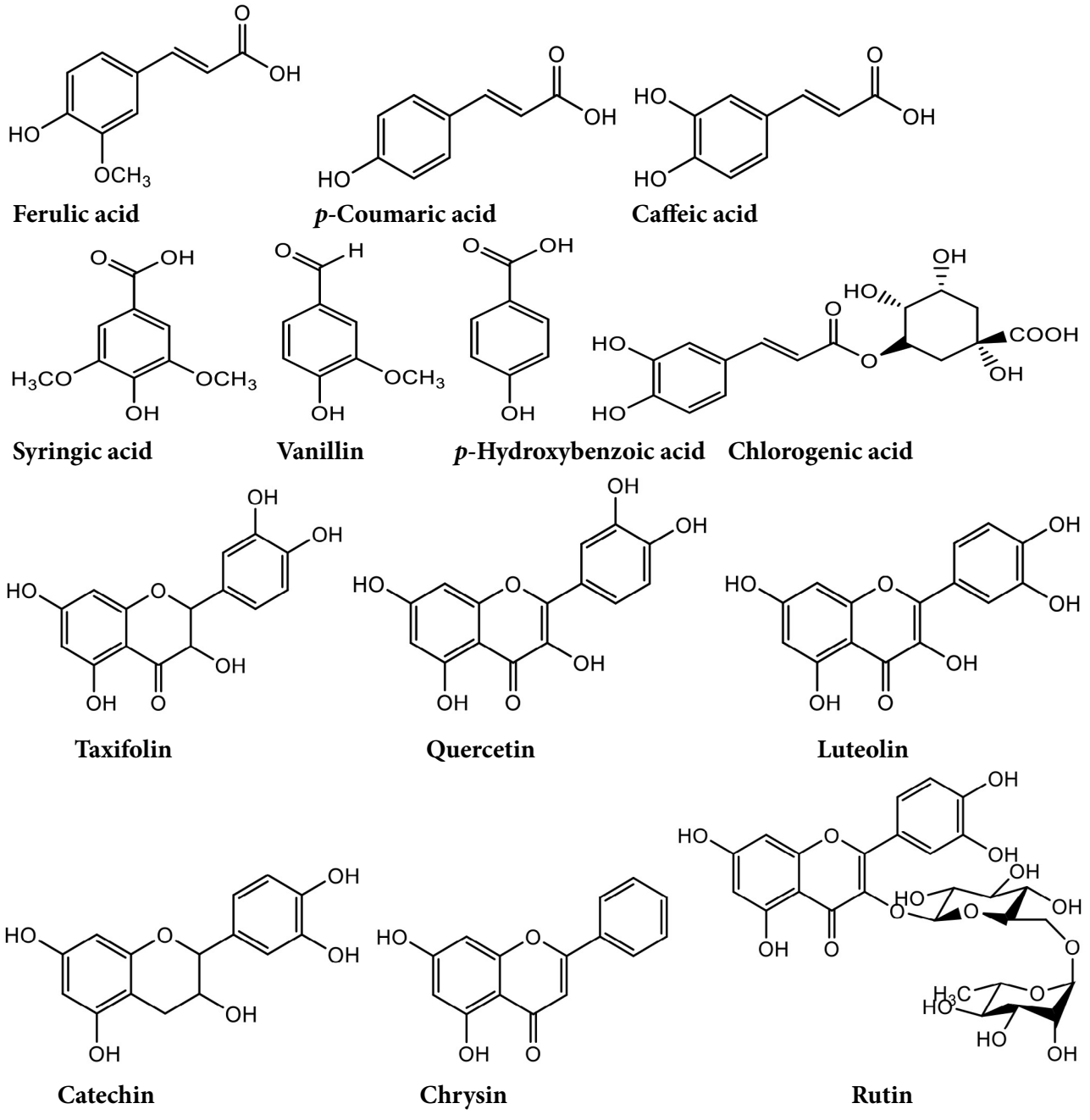

Fig. 2. Structures of the major phenolic compounds identified in *Atriplex halimus* L.

Mining dust and other contaminants, resulting from anthropogenic activities like mining can have a detrimental effect on plant phenolic compounds, perhaps lowering their levels and lowering the quality and health of the plants [34]. It has been shown that plants exposed to metal pollution tend to have low amounts of phenolic compounds as revealed through HPLC analysis of their leaf extracts [35]. Exposure to iron mining dust alters the chemical composition of *Atriplex halimus* L. Some studies illustrate the harmful effects of mine-induced air pollution on photosynthetic pigments, specifically carotenoids and total chlorophyll which reduced significantly and can slow down metabolism, plant growth and development [36]. Given the significant amount of phenolic compounds found and measured (Tables 3 and 4), these results demonstrate the effectiveness of these solvents in the extraction process. Simpler phenolic acids like p-hydroxybenzoic acid, p-coumaric acid and caffeic acid are more vulnerable to oxidative degradation due to their less complex structures [37]. Under stress, such as heavy metal exposure from mining dust, their levels decrease as plants prioritise producing more stable

Table 3. **Inhibition of violacein production against *C. violaceum* CV12472 by *Atriplex halimus* L. fractions**

Extract	MIC (mg/mL)	Violacein inhibition, %				
		MIC	MIC/2	MIC/4	MIC/8	MIC/16
W-DCM	0.625	75.2 ± 1.1	28.9 ± 0.5	15.4 ± 0.7	–	–
W-AcOEt	0.625	100 ± 0.0	80.1 ± 1.9	53.9 ± 1.1	26.6 ± 0.5	10.5 ± 0.4
W-BuOH	01.25	100 ± 0.0	49.7 ± 1.0	23.8 ± 0.1	–	–
W-Aq	01.25	100 ± 0.0	60.9 ± 0.8	34.5 ± 1.0	13.8 ± 0.4	–
T-DCM	0.625	60.1 ± 1.0	33.1 ± 1.5	11.4 ± 0.2	–	–
T-AcOEt	0.3125	100 ± 0.0	39.6 ± 2.1	17.7 ± 0.6	–	–
T-BuOH	0.625	100 ± 0.0	71.3 ± 2.6	30.9 ± 1.1	12.4 ± 0.7	–
T-Aq	0.625	100 ± 0.0	100 ± 0.0	80.6 ± 1.7	46.3 ± 1.5	28.6 ± 0.3

– : no inhibition. Values represent the means ± SEM of three measurements ($p < 0.05$).

Table 4. **Quorum sensing inhibition against *C. violaceum* CV026 by *A. halimus* fractions**

Extract	Quorum sensing inhibition zone diameters, mm				
	MIC, mg/mL	MIC	MIC/2	MIC/4	MIC/8
W-DCM	2.5	15.0 ± 0.6	09.0 ± 0.7	–	–
W-AcOEt	1.25	12.5 ± 1.0	–	–	–
W-BuOH	1.25	12.0 ± 0.6	–	–	–
W-Aq	0.625	15.0 ± 0.9	10.5 ± 0.2	–	–
T-DCM	2.5	16.0 ± 0.3	13.0 ± 0.4	09.0 ± 0.1	–
T-AcOEt	1.25	14.5 ± 0.7	11.5 ± 0.5	–	–
T-BuOH	0.625	11.0 ± 0.5	–	–	–
T-Aq	0.3125	15.5 ± 1.3	12.0 ± 0.3	08.5 ± 0.5	–

– : no inhibition. Values represent the means ± SEM of three measurements ($p < 0.05$).

and bioactive compounds [38, 39]. Syringic acid, vanillin and ferulic acid, with methoxy groups and higher antioxidant capacities, are more resistant to oxidative stress and persist under adverse conditions. These compounds are often upregulated as they provide superior defense against oxidative damage and microbial threats [40, 41]. Taxifolin, a moderately active dihydroflavonol, is susceptible to oxidation and degradation under stress [42]. In contrast, stable flavonoids like quercetin, rutin, luteolin and catechin, with higher antioxidant and protective capacities, are prioritised [43]. Plants convert intermediates like taxifolin into these products, enhancing their defense mechanisms. Overall, stress-induced metabolic reprogramming in plants shifts resource allocation towards producing complex and resilient phenolic compounds, reducing simpler precursors while ensuring effective protection against environmental stressors [34]. Environmental factors such as drought, solar radiation, rainfall and temperature are well known to strongly affect the biosynthesis of phenolic compounds in plants. Comparative interpretation with previously reported *Atriplex halimus* populations collected from Negrine, a Saharan region south of Tebessa characterised by stronger aridity and desert climatic conditions, provided important insight into the distinction between climatic and mining-associated stress responses.

The Negrine population exhibited elevated levels of compounds such as p-hydroxy benzoic acid and caffeic acid, suggesting metabolic adaptation to severe drought and desert environmental conditions. In contrast, the Ouenza population displayed markedly higher concentrations of ferulic acid, rutin, quercetin, chlorogenic acid, vanillin and catechin compared with both Tebessa and Negrine populations. These metabolites are frequently associated with antioxidant defense, reactive oxygen species scavenging, membrane stabilisation, and metal-chelating protective mechanisms under oxidative stress conditions.

Importantly, Ouenza was not the driest region among the compared sites, yet it accumulated the highest levels of several oxidative stress-related phenolic compounds, particularly ferulic acid, rutin and quercetin. If climatic drought alone explained the observed phytochemical modulation, the Saharan Negrine population would be expected to exhibit the strongest accumulation of these metabolites. However, this was not observed. These findings suggest that the metabolic profile of Atriplex halimus is influenced not only by climatic aridity but also by additional environmental pressures associated with chronic exposure to mining-derived particulate matter.

Therefore, the observed phytochemical variations should not be interpreted as random fluctuations but rather as selective metabolic reprogramming under different environmental stress conditions. While Saharan aridity mainly promoted drought-adaptive metabolites, the mining environment appeared to favour the accumulation of oxidative stress-related flavonoids and phenolic acids involved in cellular protection and stress tolerance. Our results substantiate previous studies concerning biological properties and chemical constituents of *A. halimus*. A review survey reported uses of *A. halimus* in traditional medicine, its chemical constituents including phenolic compounds as well as pharmacological activities such as antibacterial, antioxidant and antidiabetic properties [45]. Appreciable amounts of polyphenols, flavonoids, anthocyanins and tannins were described in this plant together with four flavonoids and nine phenolic acids identified and quantified using HPLC-DAD [46]. The deposition of heavy metals and particulate matter induces oxidative stress, triggering changes in the plant's secondary metabolites, particularly polyphenols and flavonoids [38]. These compounds, which play a critical role in protecting plants from oxidative damage, exhibit variations in concentration. While some polyphenols and flavonoids decrease, others increase as part of the plant's adaptive response to mitigate stress. This adjustment enhances the plant's antioxidant capacity, reflecting a shift in metabolic pathways to combat the effects of heavy metal toxicity [47]. Additionally, the absorption of iron and other metals from the dust disrupts nutrient balance, affecting overall plant health and growth [48]. These biochemical changes highlight the potential of *Atriplex halimus* L. as a bioindicator for monitoring environmental pollution and assessing the ecological impact of mining activities.

Violacein and quorum-sensing (QS) inhibition

The quorum sensing inhibition potential of plant extracts from the two regions was assessed using *C. violaceum* CV12472, a bacterium that produces purple violacein during growth, and the mutant strain *C. violaceum* CV026, which only synthesises violacein when an external acyl-homoserine lactone (AHL) is provided. The minimum inhibitory concentration (MIC) for both bacterial strains was determined, and experiments were conducted at MIC and sub-MIC levels. The findings are summarised in Table 3. The MIC values against *C. violaceum* CV12472 varied from 01.25 to 0.3125 mg/mL. For the plant sample from Ouenza, the W-AcOEt had the highest violacein inhibition that varied from 100% (MIC) to 10.5 ± 0.4% (MIC/16). For the plant sample from Tebessa, the T-Aq had the highest violacein inhibition that varied from 100% (MIC) to 28.6 ± 0.3% (MIC/16).

According to Table 3, all the extracts inhibited violacein production in *C. violaceum* CV12472 at MIC, MIC/2 and MIC/4. The violacein inhibition percentages reduced in a concentration-dependent manner. Only W-AcOEt (26.6 ± 0.5%), W-Aq (13.8 ± 0.4%), T-BuOH (12.4 ± 0.7%) and T-Aq (46.3 ± 1.5%) extracts inhibited violacein production at MIC/8. At MIC/16, only T-Aq (28.6 ± 0.3%) and W-AcOEt (10.5 ± 0.4%) extracts inhibited violacein production while the other extracts did not show any inhibition at this concentration. The MIC values against *C. violaceum* CV026 varied from 0.3125 mg/mL (T-Aq) to 2.5 mg/mL (W-DCM and T-DCM). As presented in Table 4, anti-quorum sensing zones measured in millimeters at MIC were highest in T-DCM (16.0 ± 0.3 mm) and lowest in T-BuOH (11.0 ± 0.5 mm) extract. At MIC/2, only T-DCM (13.0 ± 0.4 mm), T-Aq (12.0 ± 0.3 mm), T-AcOEt (11.5 ± 0.5 mm), W-Aq (10.5 ± 0.2 mm) and W-DCM (09.0 ± 0.7 mm) extracts have the QSI effect. With the exception of T-DCM (09.0 ± 0.1 mm) and T-Aq (08.5 ± 0.5 mm), no extracts exhibited QSI at MIC/4.

Several plant-derived molecules are known to inhibit violacein production in *Chromobacterium violaceum* CV12472 by targeting quorum sensing (QS), which regulates violacein biosynthesis [49]. These molecules interfere with QS signalling primarily by disrupting the activity of acyl-homoserine lactones

(AHLs) [50]. Interestingly, even though they contained fewer secondary metabolites, T-DCM and T-Aq extracts, among others, significantly prevented the synthesis of violacein and QS. By interfering with bacterial cell signalling pathways, especially those related to quorum sensing, this low dose and kind of polyphenols can reduce the generation of virulence factors and hinder bacterial survival. Mining iron dust influences their biosynthesis and enhances their amount, decreasing their effectiveness on QS in the Ouenza zone.

Swarming motility inhibition

Flagellated bacteria, such as *Pseudomonas aeruginosa*, use swarming movement to move across surfaces. Table 5 shows the ability of the fractions to reduce swarming movement against *P. aeruginosa*. At 100 µg/mL, all fractions W-BuOH (40.0 ± 1.2%), T-BuOH (39.3 ± 0.9%), W-Aq (34.5 ± 0.1%), W-AcOEt (32.7 ± 1.0%), T-AcOEt (30.1 ± 1.2%), T-DCM (29.0 ± 0.7%), T-Aq (25.8 ± 0.3%) and W-DCM (15.3 ± 0.5%) exhibited swarming motility inhibition. This activity reduced in a concentration-dependent manner 75 µg/mL, and only W-BuOH (10.5 ± 0.1%), T-BuOH (10.0 ± 0.6%), W-AcOEt (09.0 ± 0.5%) and W-Aq (03.0 ± 0.4%) inhibited swarming motility at 50 µg/mL. The best swarming inhibition is exhibited by the samples from the Ouenza area, specifically W-BuOH with percentage inhibitions of 40.0 ± 1.2% (100 µg/mL) and 10.5 ± 0.1% (50 µg/mL).

Reduction of swarming motility could reduce the chance of biofilm formation [51, 52]. Caffeic acid and ferulic acid are known to interfere with autoinducers (like N-acyl-homoserine lactones, which are signalling molecules in *P. aeruginosa*), leading to reduced swarming activity [53]. Quercetin has also been observed to suppress QS-regulated behaviours, making it a strong candidate for inhibiting swarming [54]. Syringic acid and rutin can affect the production or function of flagellar components, potentially leading to a weaker or less effective movement on surfaces [55, 56]. These compounds are more important in the Ouenza region due to their important production influenced by the stress of the heavy metal.

Biofilm inhibition

The MIC and anti-biofilm activity results of *Atriplex halimus* L. fractions for the considered regions are presented in Table 6. The antimicrobial activity of the samples was low to moderate and varied from 0.3125 to 5 mg/mL. The most active sample in terms of antimicrobial activity was the T-AcOEt with MIC values of 0.625, 1.25 and 0.3125 mg/mL against *S. aureus*, *E. coli* and *C. albicans*, respectively. The antibiofilm activity of the fractions was evaluated at MIC and sub-MIC concentrations. The results indicated that *S. aureus* (Gram positive bacteria) biofilms were most susceptible while *C. albicans* (fungi) biofilms were least susceptible. Overall results further indicate that the fractions from the Ouenza plant sample had higher percentage biofilm inhibitions than corresponding fractions from the Tebessa sample. Against the Gram-positive bacteria *S. aureus*, the most active fraction was W-BuOH with biofilm inhibition of 62.13 ± 1.34% (MIC) and 15.64 ± 0.22% (MIC/4). Against the Gram-negative bacteria *E. coli*, biofilm inhibition ranged from 46.24 ± 0.72% at MIC to 13.05 ± 0.2% at MIC/4 for the most active sample

Table 5. **Swarming motility inhibition on *P. aeruginosa* PA01 by *A. halimus* fractions**

Extract	Swarming inhibition, %		
	100 µg/mL	75 µg/mL	50 µg/mL
W-DCM	15.3 ± 0.5	04.9 ± 0.1	–
W-AcOEt	32.7 ± 1.0	18.2 ± 0.8	09.0 ± 0.5
W-BuOH	40.0 ± 1.2	22.5 ± 0.3	10.5 ± 0.1
W-Aq	34.5 ± 0.1	17.6 ± 0.3	03.0 ± 0.4
T-DCM	29.0 ± 0.7	13.9 ± 0.2	–
T-AcOEt	30.1 ± 1.2	15.4 ± 0.5	–
T-BuOH	39.3 ± 0.9	21.5 ± 0.7	10.0 ± 0.6
T-Aq	25.8 ± 0.3	11.2 ± 0.5	–

– : no inhibition. Values represent the means ± SEM of three measurements ($p < 0.05$).

Table 6. **MIC and anti-biofilm activity of *A. halimus* fractions**

Microorganism		W-DCM	W-AcOEt	W-BuOH	W-Aq	T-DCM	T-AcOEt	T-BuOH	T-Aq
S. aureus		0.625	1.25	2.5	1.25	1.25	0.625	1.25	0.625
E. coli		2.5	5	1.25	2.5	2.5	1.25	2.5	1.25
C. albicans		0.625	1.25	2.5	1.25	1.25	0.3125	1.25	0.625
		Biofilm inhibition, %							
S. aureus	MIC	59.31 ± 1.14	48.35 ± 0.52	62.13 ± 1.34	54.28 ± 0.69	56.6 ± 1.02	34.75 ± 0.51	55.35 ± 0.86	28.39 ± 0.20
	MIC/2	31.36 ± 0.87	21.34 ± 0.32	28.35 ± 0.85	26.58 ± 0.46	31.21 ± 0.72	12.78 ± 0.24	24.72 ± 0.38	09.16 ± 0.02
	MIC/4	13.22 ± 0.45	09.65 ± 0.08	15.64 ± 0.22	12.30 ± 0.17	19.24 ± 0.42	–	10.47 ± 0.11	–
	MIC/8	–	–	–	–	08.68 ± 0.1	–	–	–
E. coli	MIC	46.24 ± 0.72	39.50 ± 0.63	36.18 ± 0.65	25.20 ± 0.45	41.37 ± 0.86	19.34 ± 0.64	12.71 ± 0.36	10.82 ± 0.36
	MIC/2	22.26 ± 0.55	20.21 ± 0.45	23.24 ± 0.35	14.65 ± 0.23	25.36 ± 0.75	07.23 ± 0.08	–	04.52 ± 0.02
	MIC/4	13.05 ± 0.2	06.34 ± 0.2	09.85 ± 0.26	05.14 ± 0.03	08.10 ± 0.26	–	–	–
	MIC/8	–	–	–	–	–	–	–	–
C. albicans	MIC	26.27 ± 0.43	08.32 ± 0.05	–	16.22 ± 0.14	06.58 ± 0.15	31.81 ± 0.34	–	–
	MIC/2	09.94 ± 0.15	–	–	02.31 ± 0.1	–	11.28 ± 0.06	–	–
	MIC/4	–	–	–	–	–	–	–	–
	MIC/8	–	–	–	–	–	–	–	–

– : no inhibition. Values represent the means ± SEM of three measurements ($p < 0.05$).

W-DCM. For *C. albicans*, T-AcOEt (31.81 ± 0.34%), W-DCM (26.27 ± 0.43%), W-Aq (16.22 ± 0.14%), W-AcOEt (8.32 ± 0.05%), and T-DCM (6.58 ± 0.15%) extracts showed biofilm inhibition at MIC. At MIC/2, the biofilm inhibition was observed only for T-AcOEt (11.28 ± 0.06%), W-DCM (9.94 ± 0.15%) and W-Aq (2.31 ± 0.1%).

The plant *A. halimus* is described to possess antibacterial property [45]. The antimicrobial activity of various fractions of *A. halimus* vary from low to moderate. This low antimicrobial activity may be attributed to the nefarious effects of mining dust pollution on plant metabolism. However, the anti-biofilm activity of the various fractions evaluated at MIC and below MIC was good. Antibiotics which target the inhibition and death of bacterial and fungal cells are falling out of use since they are faced with resistance. Targeting microbial virulence factors like swarming, quorum-sensing and biofilm formation provide a possible solution to overcome this phenomenon [57]. Exposure to mining iron dust triggers stress responses in *Atriplex halimus* L., leading to the production of bioactive secondary metabolites such as ferulic acid, quercetin, rutin and chlorogenic acid, which inhibit biofilm formation by disrupting quorum sensing, microbial signalling, and membrane integrity [58, 59]. Compounds like taxifolin and caffeic acid suppress microbial adherence and biofilm matrix development. In *S. aureus* and *E. coli*, these compounds in Ouenza fractions can inhibit the production of autoinducers, thereby preventing biofilm maturation, and in *C. albicans*, they can block hyphal development, a key step in biofilm formation [59]. These mechanisms, combined with synergistic metabolite effects, make this plant in mining dust environments highly effective at inhibiting bacterial and fungal biofilm formation, offering promising applications in environmental and medical microbiology. Bacteria can establish biofilms on various surfaces and can float in liquid media. Since biofilms are enclosed in protective sheaths, they require higher doses of antibiotics to be eliminated, thereby constituting a great survival strategy for microorganisms [60].

Enzyme inhibition activity

The ability of the fractions in inhibiting AChE, BChE, α-glucosidase and α-amylase is reported in Table 7. The maximum test concentration was 200 µg/mL. The AcOEt fractions of both regions showed the best inhibition percentages compared to other fractions. The W-AcOEt fraction inhibited AChE and BChE

Table 7. **Anticholinesterase and antidiabetic activities of *A. halimus* fractions**

Extract/Standards	Anticholinesterase activity		Antidiabetic activity	
	AChE	BChE	α-glucosidase	α-amylase
	Inhibition, % (at 200 µg/mL)			
W-DCM	30.83 ± 0.42	38.00 ± 0.88	37.27 ± 0.15	18.70 ± 0.25
W-AcOEt	35.11 ± 0.53	52.70 ± 0.31	48.54 ± 0.85	29.47 ± 0.88
W-BuOH	21.78 ± 0.95	25.34 ± 0.52	19.27 ± 0.71	15.40 ± 0.27
W-Aq	17.95 ± 0.20	33.26 ± 0.79	22.73 ± 0.69	13.44 ± 0.88
T-DCM	23.78 ± 0.74	37.61 ± 0.31	49.41 ± 0.65	39.17 ± 0.42
T-AcOEt	31.05 ± 0.47	46.34 ± 0.86	39.82 ± 0.64	33.87 ± 0.57
T-BuOH	22.04 ± 0.44	36.67 ± 0.35	29.63 ± 0.37	22.80 ± 0.46
T-Aq	21.10 ± 0.33	27.40 ± 0.55	28.90 ± 0.55	17.63 ± 0.24
Galantamine	88.70 ± 0.50	80.20 ± 0.30	NT	NT
Acarbose	NT	NT	86.51 ± 0.45	81.33 ± 0.90

NT: not tested. Values represent the means ± SEM of three measurements ($p < 0.05$).

with percentage inhibitions of 35.11 ± 0.53% and 52.70 ± 0.31%, respectively, at 200 µg/mL. The T-AcOEt fraction showed inhibitions of 31.05 ± 0.47% and 46.34 ± 0.86% in the AChE and BChE assays, respectively. For the antidiabetic potential, the fractions W-AcOEt and T-DCM exhibited the best α-glucosidase and α-amylase inhibitions. At the highest test concentration of 200 µg/mL, W-AcOEt inhibited α-glucosidase and α-amylase with percentage inhibitions of 48.54 ± 0.85% and 29.47 ± 0.88%, respectively, while T-DCM had percentage inhibitions of 49.41 ± 0.65% and 39.17 ± 0.42% on α-glucosidase and α-amylase, respectively. The results indicate that some fraction of this plant can play a significant role in mitigating Alzheimer's disease (AD) and diabetes.

Oxidative stress, progressive neuronal degeneration, and low levels of acetylcholine characterise Alzheimer's disease (AD), one of the most prevalent forms of dementia, and visible amyloid-β deposits in the brain [61]. Inhibiting both AChE and BChE is a useful therapeutic approach to treat AD because acetylcholinesterase (AChE) and butyrylcholinesterase (BChE) typically hydrolyse acetylcholine and butyrylcholine, respectively, which lowers the neurotransmitter levels in cholinergic synapses in specific brain regions [62]. The fractions of *A. halimus* from both regions inhibited AChE with percentage inhibitions ranging from 35.11 ± 0.53% in the most active fraction to 17.95 ± 0.20% in the least active fraction. The fractions inhibited BChE to a greater extent than AChE with percentage inhibitions ranging from 52.70 ± 0.31% in the most active fraction to 25.34 ± 0.52% in the least active fraction. Methanol extract of *A. halimus* inhibited AChE with IC_{50} values p to 147.2 µg/mL [63]. This suggests that the fractions in this study were lower. Interaction with mining iron dust induces stress responses in plants, leading to the production of secondary metabolites like phenolics, flavonoids, and organic acids [38, 63]. These compounds selectively inhibit AChE, BChE and α-glucosidase due to their structural compatibility with these enzymes' active sites [64], while α-amylase, with a different site geometry, remains less affected.

Oxidative stress, type 2 diabetes (impaired glucose tolerance), hyperglycemia and dementia can also cause AD, dementia, cognitive impairment brought on by increased amyloid-beta buildup, and neuroinflammation [65, 66]. Blood glucose levels can be brought down to normal by inhibiting the enzymes (α-amylase and α-glucosidase) that break down carbohydrates to sugars [67, 68]. Several synthetic and phytochemical compounds have been used to achieve this, particularly those that can limit or stop the hydrolysis of polysaccharides like starch [69, 70]. The fractions in this study showed the potential of lowering α-amylase and α-glucosidase at 200 µg/mL up to 49.41 ± 0.65 and 39.17 ± 0.42%, respectively. *A. halimus* in a previous study was shown to possess high α-amylase inhibition and moderate α-glucosidase inhibitory effects [46]. The results of α-amylase inhibition in this study is lower than in the previous study but the α-glucosidase inhibition is almost identical. This can suggest a reduction in α-amylase inhibition, probably attributed harmful

effects upon exposure to mining iron dust. Chelation of plant metabolites by iron and the upregulation of compounds such as flavonoids and chlorogenic acid can affect the inhibition of the targeted enzymes [71, 72]. This selective response reflects adaptive strategies of the plant to environmental stress, prioritising defense mechanisms and producing less metabolites that inhibit enzymes like α-amylase. Medicinal plants that can reduce microbial infections by targeting virulence factors and also target ailments resulting from inappropriate enzymes expression are used as remedy [73]. Oxidative stress plays a major role in diabetes as well as in Alzheimer's disease and other related neurological diseases.

Antioxidant activity

In this study, cyclic voltammetry was used to test *Atriplex halimus* L. extracts from the two regions for the scavenging of superoxide radicals compared to gallic acid (GA), taken as a reference because of its interesting antioxidant properties. The oxygen behaviour measurements were conducted in a 25 mL electrochemical cell using a three-electrode system. Superoxide radical anion was generated from commercial molecular oxygen. The sweep rate was set at 100 mV/s, with the applied potential ranging from –1.6 to 0 V relative to ECS at room temperature. DMF was used as the solvent, with 0.1 M $NaBu_4NPF_6$ serving as the supporting electrolyte (Fig. 3). For oxygen

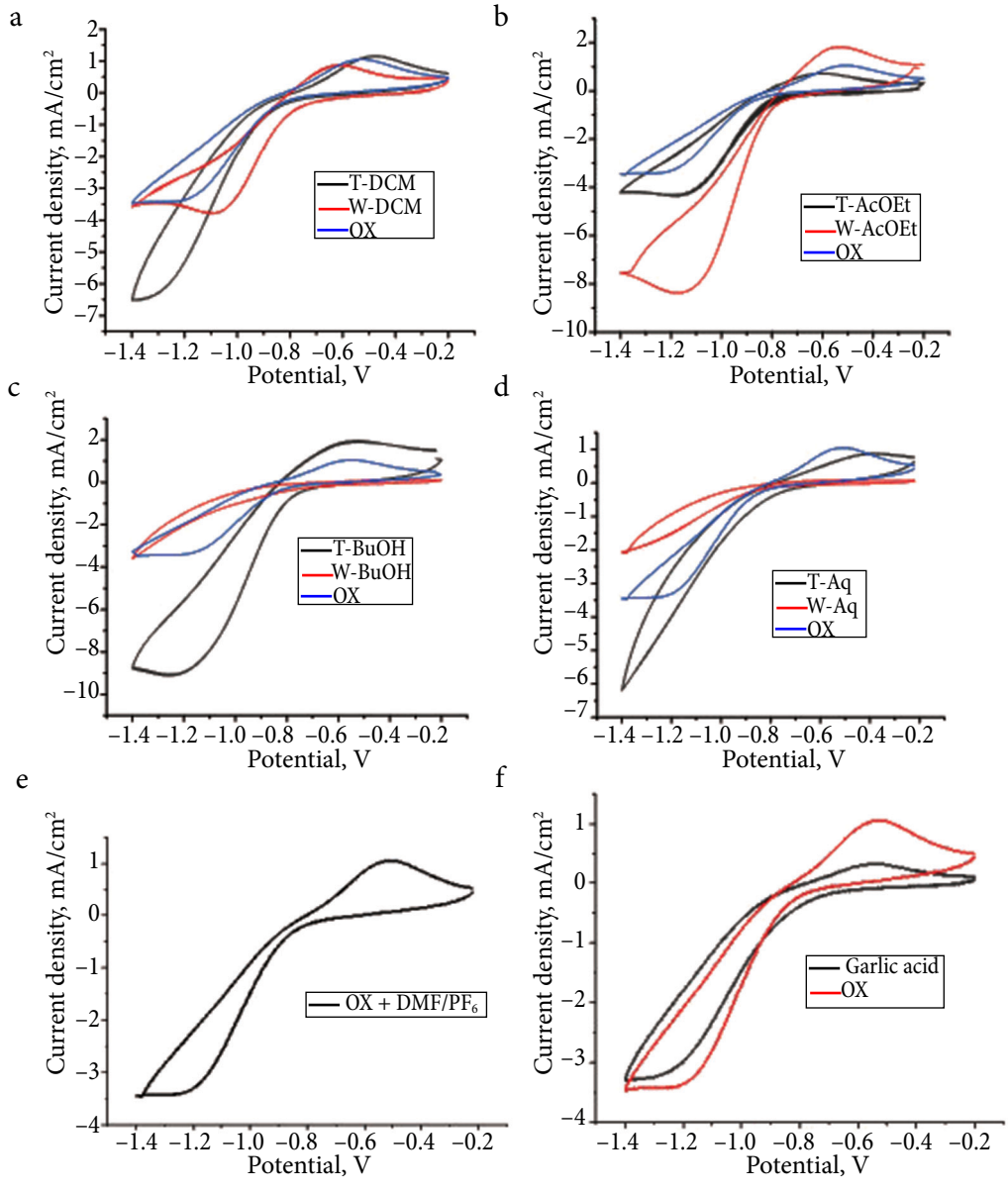

Fig. 3. Voltammograms of fractions with oxygen sparging: DCM (a), AcOEt (b), n-BuOH (c), Aq (d). Cyclic voltammogram of oxygen in DMF/PF_6 (e). Cyclic voltammograms of bubbled gallic acid and oxygen (f)

in cyclic voltammetry, the reactions typically involve the reduction and oxidation of molecular oxygen at the electrode. In an ideal reversible process, the following reactions occur. Cathodic reaction represented the reduction of oxygen. At the cathode, oxygen is reduced to form the superoxide anion (O_2^-) or other reduced species, depending on the potential applied. The main reaction at typical voltages is

$$O_2 + 2e^- \rightarrow O_2^-.$$

This reaction occurs at more negative potentials, where oxygen molecules accept electrons to form the superoxide anion. The anodic reaction represents the oxidation of oxygen. At the anode, the superoxide ion or other reduced oxygen species are oxidised back to molecular oxygen. The anodic oxidation reaction is

$$O_2^- \rightarrow O_2 + 2e^-.$$

This reaction occurs at more positive potentials, where the superoxide anion is oxidised, releasing electrons and reverting back to molecular oxygen. The general oxygen redox process involves a reversible system. The overall redox process for oxygen in a reversible cyclic voltammetry setup can be represented as

$$O_2 + 2e^- \rightleftharpoons O_2^-.$$

In this case, the oxygen molecule (O_2) is reversibly reduced to the superoxide anion (O_2^-) at the cathode and oxidised back to oxygen at the anode.

The electrochemical study of the behaviour of gallic acid with oxygen, which serves as the most potent antioxidant reference, is illustrated through the following cyclic voltammograms (Fig. 3). Gallic acid, a potent polyphenol, exhibits strong oxidation-reducing effects by scavenging reactive oxygen species (ROS) and neutralising oxidative damage. Its hydroxyl groups enable it to donate electrons or hydrogen atoms, stabilising free radicals like superoxide and hydroxyl radicals. Under the same conditions as previously described, a precise amount of *Atriplex halimus* L. extract (0.0178 mg dissolved in 20 mL of solvent) was introduced into the electrochemical cell. The resulting cyclic voltammograms (Fig. 3) correspond to various oxygen-bubbled plant fractions. The calculated percentages of the superoxide anion inhibition by the standard antioxidant (gallic acid), as well as the studied extracts, are grouped in Table 8.

According to the results in Table 8, it is suggested that gallic acid gives a good inhibition of superoxide radicals, with a percentage of 73.85%. Among the *Atriplex halimus* L. fractions, the Ouenza extracts showed the highest percentage inhibition, with the W-Aq extract achieving 98.98% inhibition and the W-BuOH extract reaching 94.84%. This suggests that these extracts contain molecules with hydroxyl groups involved in the inhibition process. Intracellular oxidative stress arises due to the imbalance in the production of reactive oxygen/reactive nitrogen species and cellular antioxidant defense mechanisms. The renewal of the body's human cells is a continuous metabolite transformation during our lives. This process causes oxidation, leading to free radicals, usually superoxide molecules that seek to fuse with other entities to complement each other [74]. In addition to this natural phenomenon in the human body, other sources of free radicals come from food, radiation and pollution [75].

Table 8. **Percentages of superoxide ion inhibition**

	I_a, mA/cm^2		*E*, V		Inhibition, %	
O_2	01.0521		–00.5043		/	
GA	00.2751		–00.5188		73.85	
Extracts	W	T	W	T	W	T
DCM	00.7952	01.1439	–00.6320	–00.4790	24.42	(hp)
AcOEt	01.8059	00.7163	–00.5260	–00.5970	(hp)	31.92
BuOH	00.0543	01.8717	–00.5090	–00.5520	94.84	(hp)
Aq	00.0107	00.8832	–00.6110	–00.3740	98.98	16.05

(hp): higher percentage.

These unstable entities are at the origin of the cell's aging, the organ's hardening causing the appearance of cancers, as well as many other diseases [76, 77]. The human body produces its own enzymatic and non-enzymatic antioxidants, but the nutritional intake rich in antioxidants of vegetable origin is one of the major assets of protection against these radicals [78, 79]. Various methods can evaluate the antioxidant activity of medicinal plants, including cyclic voltammetry, which is an electrochemical method to characterise oxidisable and reducible compounds in a solution. The antioxidant activity of natural extracts was linked to the redox comportment of polyphenol substituents (-OH), expressed by oxidation pics (intensity (Ia) and potential (Ea)) and reduction pics if the system was reversible [80]. The W-Aq extract contains ferulic acid in the highest concentration, a compound known for its strong ability to neutralise reactive oxygen species (ROS), thereby reducing oxidative damage [81]. Similarly, the W-BuOH extract contains both ferulic acid and quercetin in high concentrations. In addition to the effects of ferulic acid, quercetin exhibits a high capacity to donate hydrogen atoms, directly scavenging free radicals such as superoxide anions and hydroxyl radicals [82]. Furthermore, quercetin can chelate metal ions like iron, which catalyse ROS production, thereby preventing oxidative chain reactions [83, 84]. In contrast, the Tebessa extracts did not exhibit a significant inhibitory activity. The W-AcOEt, T-DCM and T-BuOH extracts exhibited higher current values than oxygen, suggesting that these fractions likely contain multiple oxidisable molecules capable of producing a greater quantity of free radicals than oxygen. In the presence of excess iron, quercetin may contribute to the redox cycling of iron, potentially leading to localised radical generation [85]. This study confirms the previous study about *A. halimus* from two geo-climatic zones of Algeria which were shown to contain phenolic compounds and exhibited anticholinesterase, antidiabetic, antibiofilm and anti-quorum-sensing properties [86].

CONCLUSIONS

In conclusion, the study highlights the significant role of phenolic compounds in the response of *Atriplex halimus* L. to environmental stress caused by mining iron dust. The results demonstrate that certain phenolic acids, such as caffeic acid, ferulic acid, quercetin and rutin, exhibit strong antioxidant and antimicrobial properties, particularly in inhibiting biofilm formation and disrupting quorum sensing in bacteria and fungi. These compounds increase under stress conditions, highlighting the plant's adaptive strategy to mitigate oxidative damage and microbial threats. Interestingly, while some compounds like p-hydroxybenzoic acid are more susceptible to oxidative degradation, others, like syringic acid and vanillin, are more resilient and contribute to the plant's defence mechanisms. The extracts from the plant also demonstrated a significant antibacterial and anti-quorum sensing activity, with T-DCM and T-Aq extracts, in particular, showing a strong inhibition of violacein production in *Chromobacterium violaceum* CV12472. The interaction with mining iron dust enhanced the production of bioactive secondary metabolites, which may alter bacterial signalling pathways, offering potential applications in both environmental and medical microbiology. Furthermore, the plant's ability to selectively inhibit enzymes such as AChE, BChE and α-glucosidase while leaving α-amylase less affected reflects its evolved defence mechanisms in response to heavy metal stress.

The present study demonstrates that the phytochemical composition and biological activities of *Atriplex halimus* L. are strongly influenced by environmental conditions. Comparative analysis between Tebessa City, Ouenza, and previously reported Saharan populations from Negrine suggests that different environmental pressures induce distinct metabolic adaptation patterns. While Saharan aridity mainly promoted drought-associated metabolites, the mining-area population from Ouenza exhibited a selective enrichment in oxidative stress-related flavonoids and phenolic acids such as ferulic acid, rutin, quercetin, chlorogenic acid and catechin. These findings indicate that the metabolic modulation observed in Ouenza cannot be explained solely by climatic drought, since the Saharan Negrine population was exposed to stronger aridity but did not exhibit similar accumulation patterns for several oxidative stress-related metabolites. Therefore, the observed phytochemical and biological changes likely result from combined environmental pressures,

including semi-arid climatic conditions and chronic exposure to mining-derived particulate matter. The results further support the hypothesis that mining-associated oxidative stress contributes significantly to the adaptive metabolic reprogramming of *Atriplex halimus*. These suggest that *Atriplex halimus* L. could be a valuable resource for developing natural bioactive compounds to combat microbial biofilms and oxidative stress in mining-impacted environments.

Received 15 March 2026
Accepted 28 May 2026

References

1. M. A. Murzin, N. V. Gorlenko, *IOP Conf. Ser.: Earth Environ. Sci.* **677**, 042091 (2021) [https://doi.org/10.1088/1755-1315/677/4/042091].
2. N. Kayet, K. Pathak, C. P. Singh, R. K. Chaturvedi, A. S. V. Brahmandam, C. Mandal, *J. Environ. Manag.*, **367**, 121935 (2024).
3. N. Tarannum, N. Rathore, A. Natwadiya, et al., *Environ. Sci. Pollut. Res.*, **31**, 33515 (2024) [https://doi.org/10.1007/s11356-024-33449-w].
4. M. Matsuki, M. R. Gardener, A. Smith, R. K. Howard, A. Gove, *Austral Ecol.*, **41(4)**, 417–427 (2016) [https://doi.org/10.1111/aec.12328].
5. A. D. Watkinson, J. Virgl, V. S. Miller, et al., *J. Environ. Qual.*, **50(4)**, 990 (2021) [https://doi.org/10.1002/jeq2.20251].
6. M. E. Boi, M. Fois, L. Podda, M. Porceddu, G. Bacchetta, *Plants*, **12(22)**, 3823 (2023) [https://doi.org/10.3390/plants12223823].
7. N. Abederahmane, L. Khochemane, L. Gadri, K. Rais, O. Bennis, *Min. Sci.*, **25**, 19 (2018) [https://doi.org/10.5277/msc182503].
8. R. Chafika, D. G. Amara, *Int. J. Health Sci.*, **8(1)**, 1 (2023) [https://doi.org/10.53730/ijhs.v8n1.14642].
9. N. Benhammou, F. A. Bekkara, T. K. Panovska, *Chimie*, **12(12)**, 1259 (2009) [https://doi.org/10.1016/j.crci.2009.02.004].
10. L. Ziane, A. Berreghioua, M. Djellouli, *AJCBR*, **6(2)** (2023).
11. K. Zeghib, D. A. Boutlelis, *Iran. J. Pharm. Res.*, **20(1)**, 296 (2021) [https://doi.org/10.22037/ijpr.2020.111634.13272].
12. Z. Khaoula, B. D. Ali, *J. Drug Deliv. Ther.*, **10(3)**, 217 (2020).
13. M. K. Parvez, A. H. Arbab, M. S. AlDosari, et al., *Exp. Ther. Med.*, **15(4)**, 3883 (2018) [https://doi.org/10.3892/etm.2018.5919].
14. S. Sai Kachout, A. Ennajah, K. Guenni, N. Ghorbel, A. Zoghlami, *Soil Sediment Contam.*, **33(2)**, 139 (2024) [https://doi.org/10.1080/15320383.2023.2185469].
15. S. Ishtiyaq, H. Kumar, R. J. D'Souza, M. Varun, P. J. Favas, M. S. Paul, *Soil Syst.*, **7(2)**, 46 (2023) [https://doi.org/10.3390/soilsystems7020046].
16. B. Amaria, B. Djilali, S. M. Abdesselem, L. Brahim, *SAJEB*, **10(6)**, 383 (2020) [https://doi.org/10.38150/sajeb].
17. K. Rais, R. Hadji, L. Boudiba, et al., *Min. Miner. Deposits*, **19(3)**, 98 (2025) [https://doi.org/10.33271/mining19.03.098].
18. Z. Wang, W. Zhou, I. M. Jiskani, H. Luo, Z. Ao, E. M. Mvula, *Sci. Total Environ.*, **825**, 153949 (2022).
19. N. Haque, *InIron Ore*, 691, (2022) [https://doi.org/10.1016/j.scitotenv.2022.153949].
20. O. Zerzour, L. Gadri, R. Hadji, F. Mebrouk, Y. Hamed, *Geotech. Geol. Eng.*, **39(5)**, 3337 (2021).
21. M. Gabarrón, R. Zornoza, J. A. Acosta, Á. Faz, S. Martínez-Martínez, *Adv. Chem. Pollut. Environ. Manag. Protect.*, **4**, 157 (2019) [https://doi.org/10.1016/bs.apmp.2019.07.003].
22. B. Paluchamy, D. P. Mishra, D. C. Panigrahi, *J. Clean. Prod.*, **296**, 126524 (2021) [https://doi.org/10.1016/j.jclepro.2021.126524].
23. F. Anlimah, V. Gopaldasani, C. MacPhail, B. Davies, *Environ. Sci. Pollut. Res. Int.*, **30(19)**, 54407 (2023) [https://doi.org/10.1007/s11356-023-26321-w].
24. S. Boudiba, S. Kucukaydin, A. N. Tamfu, et al., *Pharmacogn. Res.*, **15(2)**, 373 (2023).
25. C. Haouam, S. Boudiba, A. N. Tamfu, et al., *Plants*, **12(24)**, 4134 (2023) [https://doi.org/10.3390/plants12244134].
26. A. N. Tamfu, O. Ceylan, G. Cârâc, E. Talla, R. M. Dinica, *Molecules*, **27(15)**, 4872 (2022) [https://doi.org/10.3390/molecules27154872].
27. M. Popova, D. Gerginova, B. Trusheva, et al., *Foods*, **10(5)**, 997 (2021) [https://doi.org/10.3390/foods10050997. https://doi.org/10.3390/foods10050997].
28. S. Boudiba, A. N. Tamfu, B. Berka, et al., *Nat. Prod. Commun.*, **16(6)**, 1934578X211024039 (2021) [https://doi.org/10.1177/1934578X211024039].
29. A. N. Tamfu, G. Kocak, O. Ceylan, F. Valentine, V. Bütün, H. Çiçek, *J. Appl. Polym. Sci.*, **140(11)**, e53631 (2023).
30. R. T. Feunaing, A. N. Tamfu, A. J. Y. Gbaweng, et al., *Molecules*, **29**, 2456 (2024) [https://doi.org/10.3390/molecules29112456].
31. A. N. Tamfu, O. Ceylan, S. Kucukaydin, M. E. Duru, *LWT*, **133**, 110150 (2020) [https://doi.org/10.1016/j.lwt.2020.110150].
32. M. M. Quradha, M. E. Duru, S. Kucukaydin, et al., *Sci. Rep.*, **14(1)**,1885 (2024).
33. M. Hani, C. Boubekri, T. Lanez, *AJRC*, **16(1)**, 18 (2023) [https://doi.org/10.52711/0974-4150.2023.00004].
34. N. Vinogradova, E. Vinogradova, V. Chaplygin, et al., *Molecules*, **28(17)**, 6322 (2023) [https://doi.org/10.3390/molecules28176322].

35. B. Márquez-García, M. Á. Fernández, F. Córdoba, *Bioresour. Technol.*, **100(1)**, 446 (2009) [https://doi.org/10.1016/j.biortech.2008.04.070].
36. A. Gupta, S. K. Sharma, A. Mishra, et al., *Vegetos*, **37**, 1833 (2024) [https://doi.org/10.1007/s42535-024-00992-3].
37. A. P. Da Silva, W. G. Sganzerla, O. D. John, R. Marchiosi, *Phytochem. Rev.*, 1 (2023).
38. D. M. Asiminicesei, D. I. Fertu, M. Gavrilescu, *Plants*, **13(6)**, 913 (2024) [https://doi.org/10.3390/plants13060913].
39. I. Mirkov, D. Stojković, A. P. Aleksandrov, et al., *Curr. Pharm. Des.*, **26(16)**, 1799 (2020) [https://doi.org/10.2174/1381612826666200407163408].
40. V. D. Kancheva, M. A. Dettori, D. Fabbri, et al., *Antioxidants*, **10(4)**, 624 (2021) [https://doi.org/10.3390/antiox10040624].
41. P. Tuladhar, S. Sasidharan, P. Saudagar, *Biocontrol Agents and Secondary Metabolites*, 419, Woodhead Publishing (2021) [https://doi.org/10.1016/B978-0-12-822919-4.00017-X].
42. J. Laoué, C. Fernandez, E. Ormeño, *Plants*, **11(2)**, 172 (2022) [https://doi.org/10.3390/plants11020172].
43. B. Akbari, N. Baghaei-Yazdi, M. Bahmaie, F. Mahdavi Abhari, *BioFactors*, **48(3)**, 611 (2022) [https://doi.org/10.1002/biof.1831].
44. H. Samsami, R. Maali-Amiri, *Plant Physiol. Biochem.*, 108862 (2024) [https://doi.org/10.1016/j.plaphy.2024.108862].
45. M. Roubi, M. Dalli, S. E. Azizi, N. Gseyra, *Chem. Biodivers.*, e202402171 (2024) [https://doi.org/10.1002/cbdv.202402171].
46. M. M. Guedri, N. Krir, C. C. Terol, M. Romdhane, A. Boulila, A. Guetat, *Chem. Biodivers.*, **21(7)**, e202301941 (2024) [https://doi.org/10.1002/cbdv.202301941].
47. I. Noor, H. Sohail, J. Sun, M. A. Nawaz, G. Li, M. Hasanuzzaman, J. Liu, *Chemosphere*, **303**, 135196 (2022) [https://doi.org/10.1016/j.chemosphere.2022.135196].
48. S. Kameswaran, Y. Gunavathi, P. G. Krishna, *RJLBPCS*, **5(1)**, 341 (2019) [https://doi.org/10.26479/2019.0501.31].
49. P. D. Dimitrova, T. Damyanova, T. Paunova-Krasteva, *Sci. Pharm.*, **91(3)**, 33 (2023) [https://doi.org/10.3390/scipharm91030033].
50. A. Hartmann, S. Klink, M. Rothballer, *Pathogens*, **10(12)**, 1561 (2021) [https://doi.org/10.3390/pathogens10121561].
51. A. N. Tamfu, O. Ceylan, G. C. Fru, M. Ozturk, M. E. Duru, F. Shaheen, *Microb. Pathog.*, **144**, 104191 (2020 Jul) [https://doi.org/10.1016/j.micpath.2020.104191].
52. S. Boudiba, A. N. Tamfu, K. Hanini, et al., *J. Chem. Res.*, **47(4)**, 17475198231184603 (2023).
53. A. Bouyahya, I. Chamkhi, A. Balahbib, et al., *Molecules*, **27(5)**, 1484 (2022) [https://doi.org/10.3390/molecules27051484].
54. S. Kameswaran, B. Ramesh, in: *Quorum Quenching: A Chemical Biological Approach for Microbial Biofilm Mitigation and Drug Development*, Ch. 5, Royal Society of Chemistry (2023) [https://doi.org/10.1039/BK9781837671380-00105].
55. S. S. Nassarawa, G. A. Nayik, S. D. Gupta, et al., *Crit. Rev. Food Sci. Nutr.*, **63(28)**, 9482 (2023) [https://doi.org/10.1080/10408398.2022.2067830].
56. L. N. Silva, K. R. Zimmer, A. J. Macedo, D. S. Trentin, *Chem. Rev.*, **116(16)**, 9162 (2016) [https://doi.org/10.1021/acs.chemrev.6b00184].
57. R. M. Talla, A. N. Tamfu, B. N. K. Wakeu, et al., *BMC Complement. Med. Ther.*, **23(1)**, 300 (2023) [https://doi.org/10.1186/s12906-023-04115-4].
58. M. Ivanov, K. Novović, M. Malešević, et al., *Pharmaceuticals*, **15(3)**, 385 (2022) [https://doi.org/10.3390/ph15030385].
59. M. Rudrapal, B. Sarkar, P. Deb, A. Bendale, A. Nagar, in: *Polyphenols: Food, Nutraceutical, and Nanotherapeutic Applications*, Ch. 13, Wiley (2023) [https://doi.org/10.1002/9781394188864.ch13].
60. A. Benaissa, B. Wafaa, A. Ngenge Tamfu, et al., *Chem. Biodivers.*, e202402693 (2024) [https://doi.org/10.1002/cbdv.202402693].
61. A. N. Tamfu, S. Kucukaydin, B. Yeskaliyeva, M. Ozturk, R. M. Dinica, *Molecules* **26**, 5582 (2021) [https://doi.org/10.3390/molecules26185582].
62. M. J. Uddin, D. Russo, M. M. Rahman, et al., *Evid. Based Complement. Alternat. Med.*, **2021**, 9995614 (2021) [https://doi.org/10.1155/2021/9995614].
63. P. Alugoju, T. Tencomnao, *Plants and Their Interaction to Environmental Pollution*, 379, Elsevier (2023) [https://doi.org/10.1016/B978-0-323-99978-6.00018-2].
64. G. Zengin, N. M. Fahmy, K. I. Sinan, et al., *Processes,* **10(10)**, 1911 (2022) [https://doi.org/10.3390/pr10101911].
65. Z. Breijyeh, R. Karaman, *Molecules*, **25**, 5789 (2020) [https://doi.org/10.3390/molecules25245789].
66. A. N. Tamfu, N. Roland, A. M. Mfifen, et al., *Arab. J. Chem.*, **15(4)**, 103675 (2022).
67. T. D. Tran, V. L. Tu, T. M. Hoang, et al., *Cureus*, **15(4)**, e37267 (2023) [https://doi.org/10.7759/cureus.37267].
68. N. T. Metiefeng, A. N. Tamfu, M. Fotsing Tagatsing, et al., *Molecules* **28**, 4802 (2023) [https://doi.org/10.3390/molecules28124802].
69. A. M. Munvera, T. Alfred Ngenge, B. M. W. Ouahouo, et al., *Nat. Prod. Res.*, **37(24)**, 4169 (2023) [https://doi.org/10.1080/14786419.2023.2176491].
70. S. Luo, L. Zhao, H. Peng, Z. Peng, G. Wang, *Eur. J. Med. Chem.*, **275**, 116600 (2024) [https://doi.org/10.1016/j.ejmech.2024.116600].
71. A. Scarano, B. Laddomada, F. Blando, et al., *Antioxidants*, **12(3)**, 630 (2023) [https://doi.org/10.3390/antiox12030630].
72. A. Benaissa, A. N. Tamfu, S. Boudiba, et al., *Nat. Prod. Commun.* **20(2)**, 1934578X251314357 (2025).

73. V. Sharma, M. M. Mehdi, *Neurochem. Int.*, **164**, 105490 (2023) [https://doi.org/10.1016/j.neuint.2023.105490].
74. V. Lobo, A. Patil, A. Phatak, N. Chandra, *Pharmacogn. Rev.*, **4(8)**, 118 (2010) [https://doi.org/10.4103/0973-7847.70902].
75. I. Z. Sadiq, *Curr. Mol. Med.*, **23(1)**, 13 (2023) [https://doi.org/10.2174/1566524022666211222161637].
76. A. Phaniendra, D. B. Jestadi, L. Periyasamy, *Indian J. Clin. Biochem.*, **30**, 11 (2015).
77. İ. Gulcin, *Arch. Toxicol.*, **94(3)**, 651 (2020).
78. A. B. Amira Semchaoui, *Evaluation des activités biologiques d'une plante médicinale* (*Peganum harmala* L.), Doctoral Dissertation (2021).
79. H. F. Zohra, B. Sameh, B. Louiza, et al., *Biochem. Res. Int.*, **2025(1)**, 6238789 (2025).
80. H. Hotta, H. Sakamoto, S. Nagano, T. Osakai, Y. Tsujino, *Biochim. Biophys. Acta*, **1526(2)**, 159 (2001) [https://doi.org/10.1016/S0304-4165(01)00123-4].
81. A. Amić, Z. Marković, J. M. Marković, D. Milenković, V. Stepanić, *Phytochemistry*, **170**, 112218 (2020) [https://doi.org/10.1016/j.phytochem.2019.112218].
82. B. Kaurinovic, D. Vastag, *IntechOpen* (2019) [https://dx.doi.org/10.5772/intechopen.83731].
83. Z. Kejík, R. Kaplánek, M. Masařík, et al., *Int. J. Mol. Sci.*, **22(2)**, 646 (2021) [https://doi.org/10.3390/ijms22020646].
84. İ. Gulcin, S. H. Alwasel, *Processes*, **10(1)**, 132 (2022) [https://doi.org/10.3390/pr10010132].
85. M. Leopoldini, N. Russo, S. Chiodo, M. Toscano, *J. Agric. Food Chem.*, **54(17)**, 6343 (2006) [https://doi.org/10.1021/jf060986h].
86. A. Baccouche, S. Boudiba, B. Berka, et al., *Chem. Pap*. (2025) [https://doi.org/10.1007/s11696-025-04314-y].

Khaled Rais, Louiza Boudiba, Sameh Boudiba,
Alfred Ngenge Tamfu, Baya Berka,
Selcuk Kucukaydin, Ozgur Ceylan, Karima Hanini

LYGINAMASIS *ATRIPLEX HALIMUS* L. (AMARTHACEAE) FENOLIŲ SUDĖTIES, FERMENTŲ SLOPINIMO, ANTIMIKROBINIO VIRULENTIŠKUMO IR CHEMINIO ANTIOKSIDACINIO AKTYVUMO ĮVERTINIMAS IŠ KASYBOS IR NE KASYBOS VIETŲ RYTŲ ALŽYRE